IEEE Access
Multidisciplinary | Rapid Review | Open Access Journal

Received May 13, 2022, accepted May 24, 2022, date of publication May 30, 2022, date of current version June 9, 2022.

Digital Object Identifier 10.1109/ACCESS.2022.3178692

A Condition Monitoring Strategy of Looms Based on DSmT Theory and Genetic Multiobjective Optimization Improves the Rough Set Method

WEILING LIU, PING LIU, XIAOLIANG WANG, ZHAOZONG MENG, (Member, IEEE), YUNFENG JIANG, AND YANJUN XIAO

School of Mechanical Engineering, Hebei University of Technology, Tianjin 300401, China

Corresponding author: Yanjun Xiao (xyj_hebut@163.com)

ABSTRACT In order to improve the effect of intelligent monitoring and condition analysis of textile machinery, some solutions have been proposed to mitigate incomplete monitoring positions, insufficient decision accuracy, uncertainty reasoning and generalization of the current loom monitoring system. Firstly, a model of the weaving machine spindle dynamics was constructed, and the types and sources of monitoring data were specified. Secondly, an improved rough set method is proposed for processing the collected loom attribute data. A genetic multi-objective optimization method combined with a genetic algorithm is proposed to improve the problem of too many reduction results of the rough set method and improve the monitoring system's reliability. In order to solve the problem that new objects do not have unique matching rules in the constructed rule base, a fusion of Dezert-Smarandache Theory (DSmT) for uncertainty inference is proposed, which increases the distinguishability of decision support probabilities. Experiments show that the improved rough set method based on DSmT and genetic multi-objective optimization has higher classification accuracy and better recognition than the traditional rough set method for weaving machine condition monitoring.

INDEX TERMS Genetic algorithm, rapier loom, rough set, uncertainty reasoning.

I. INTRODUCTION

Condition monitoring and identification of textile machinery is the basis for the digitalization and intelligence of textile machinery. With the continuous development of textile machinery functions and structures, traditional equipment condition monitoring technology cannot meet the needs of intelligent weaving equipment. Therefore, a particular loom condition monitoring method is studied. It is an inevitable choice and an essential direction for the current development of textile machinery. Equipment maintenance technology has gone through four stages: post-event maintenance, preventive planned maintenance, maintenance considering economic goals, and condition maintenance. The innovation of each generation of equipment maintenance technology is actually the innovation of equipment condition monitoring technology. With the development of deep learning and multi-source data fusion, the current equipment condition monitoring technology is no longer limited to equipment maintenance. It is based on the hidden state information inside the equipment so as to realize intelligent manufacturing applications such as intelligent fault warning, intelligent efficiency optimization, and CPS model mapping of equipment.

The associate editor coordinating the review of this manuscript and approving it for publication was Hisao Ishibuchi.

A. DEVELOPMENT STATUS OF LOOM MONITORING SYSTEM

DORNIER's loom control system adopts industrial interconnection technology, which can precisely control and monitor the critical quality parameters of the loom. The Picanol BlueBox, an electronic platform for looms from Picanol, Belgium, integrates on-board diagnostic systems, intelligent production efficiency optimization systems, user interfaces, device browsers, and remote fault diagnosis systems. It better realizes the loom's innovative management and online fault diagnosis [1]. Vladimir *et al.* built a fabric visual inspection

system through a web camera and a microcomputer and designed a feasible scheme for automatic online monitoring of fabric quality [2]. P. P. J designed a shuttle loom control module with the peripheral interface and microcontroller, which can monitor and measure errors in warp and weft [3].

Dong and Shi adopted the redundant structure of dual-bus and dual-region processors to realize the self-diagnosis of the loom system, the automatic loading of working parameters, and the automatic shielding and recovery of loom interface faults. This system has high reliability and maintainability, but the degree of intelligence is insufficient [4]. Sun *et al.* used the fault tree to judge the real-time data, which improved the data transmission and processing performance of the real-time information detection system of the loom [5]. The above works have designed the control and monitoring system of the loom, but these systems have the problem of insufficient intelligence. The focus of these researches does not involve data fusion and feature extraction of loom attributes, loom status recognition and loom data sharing. In order to realize the condition monitoring of the loom, it is necessary to analyze the entire mechanical structure of the loom, establish a dynamic model of the core components of the loom, and determine the data source and data type of the loom monitoring data according to the model. It is also necessary to analyze a large amount of data collected by combining intelligent condition monitoring methods and fault diagnosis methods to support the system in making correct decisions.

B. DEVELOPMENT STATUS OF CONDITION MONITORING AND FAULT DETECTION TECHNOLOGY

The new state monitoring system typically includes data acquisition, analysis; diagnosis and output; data transmission; and communication [6]–[10]. Existing condition monitoring systems typically replace single-sensor signal monitoring with multisensor data fusion monitoring. Caporuscio *et al.* analyzed troubleshooting solutions for many heterogeneous connected devices and summarized the effect evaluation criteria of status detection and fault diagnosis systems from different perspectives [11]. Reference [12] comprehensively used multiple sensor signals to construct a health monitoring and fault diagnosis system for hydromechanical transmission. Experiments proved that the condition monitoring method based on multisensor data fusion has lower hysteresis and a more accurate condition recognition effect than the traditional ferrography analysis and vibration monitoring methods. In power systems, condition monitoring technology has matured in many applications, and there is a separate online condition monitoring method for each device in the system [13]–[15]. It can be seen that the specificity of the condition monitoring technology is very high, the condition monitoring of different manufacturing equipment needs to be studied in a targeted manner, and the monitoring points and data volume of the condition monitoring task are massive. A more efficient data processing method is needed. The set and data sharing requirements are higher [16], [17]. In the field of condition monitoring systems, the research on algorithms for mining deep hidden information combined with deep learning methods has become a hot topic. Reference [18] proposed using the fuzzy threshold method to classify the state data of wind turbines and then using the fuzzy neural network (FNN) and fast Fourier transform to evaluate and make decisions about monitoring data. Reference [19] proposed using likelihood learning to process the warpage feature of the wind turbine gearbox vibration signal. These cases show that algorithms such as deep learning can effectively mine deeply hidden information in state data but are strongly dependent on the dataset.

How to quickly obtain high-quality condition monitoring data sets and improve the generalization performance of control decisions is a practical problem that needs to be faced. Chen constructed a wavelet neural network algorithm based on the niche genetic algorithm for fault diagnosis of rapier loom bearings [20]. Zhang *et al.* proposed a grid fault localization and fault type identification method that combines Variational Mode Decomposition (VMD) and Convolutional Neural Networks (CNN) [21]. Zhang *et al.* proposed using a multi-group quantum genetic algorithm (MQGA) to optimize the combination of quality factor parameters for fault detection of aero-engine bearings [22]. Zhang *et al.* proposed using deep convolution generative adversarial network (DCGAN) to generate virtual fault data, expand the training samples, and then use the residual connected convolutional neural network (RCCNN) model to extract and classify stator current data to achieve fault diagnosis [23]. The above works have proposed different fault diagnosis and condition monitoring methods. However, the above work has a general effect of dealing with uncertain information with complex data sources. It is not suitable for the loom system in which each institution's data is relatively independent, and a consistent interpretation and description of the equipment status cannot be obtained. In order to improve the processing effect of multi-source uncertain information, it is necessary to introduce multi-source data fusion technology, such as rough set theory, grey system theory, Bayesian reasoning, etc.

Rough set theory (RST) has been successfully applied to machine learning, decision analysis, process control, approximate reasoning, pattern recognition, data mining and other intelligent information processing fields. Zhang *et al.* discussed the methods and applications of multisource information fusion based on rough set theory, reporting that rough sets are suitable for classifying noisy, inaccurate, or incomplete data [24]. RST does not rely on prior information. It can make full use of available information to identify basic knowledge and rules of target problems from sample data to keep the classification ability of the information system unchanged [25]. Muralidharan *et al.* proposed using a discrete wavelet transform (DWT) to calculate wavelet features from vibration signals and then using rough set generation rules to achieve fault diagnosis of single-body centrifugal pumps [26]. Wang *et al.* proposed a fault diagnosis scheme combining rough set theory and fuzzy logic [27].

These examples show that using the rough set method to process data can extract effective decision-making rules from data with complex sources and ambiguous relationships. However, the rules extracted by the simple rough set method may have new objects that cannot be matched. Therefore, it is necessary to integrate other suitable algorithms to improve the accuracy and adaptability of the constructed decision rule base. The steps of the rough set method include attribute reduction, rule extraction, and rule matching. Some scholars propose integrating other algorithms to improve the results of these steps to improve decision-making using the rough set method. For example, Suo *et al.* proposed using a data-driven loss function matrix to design a neighbourhood decision theory rough set model to improve the results of attribute reduction [28]. Rajeswari *et al.* proposed using a genetic algorithm (GA) and a rough set-based method to select the best input features to improve the reduction efficiency [29]. Hu *et al.* introduce different weights into neighbourhood relations and construct a Weighted Neighborhood Rough Set (WNRS) model based on weighted neighbourhood relations. The experimental results show that WNRS has higher classification accuracy and compression ratio [30]. Xie *et al.* propose a new weighted neighbourhood probabilistic rough set model based on data binning [31]. Although the above work improves the rough set method, it is not entirely suitable for processing loom attribute data. The state data of the loom is continuous in the time domain, which cannot be processed by the rough set method. In addition, the above work mainly improves the attribute reduction step of the rough set method, and the rule extraction step and the rule matching step of the rough set method are less improved. When the rough set method processes the loom state data, there are many reduction results, and the new object cannot match the unique rule in the rule base. In order to solve these two problems, this paper proposes to use the genetic algorithm to improve the attribute reduction step of the rough set method so as to improve the classification accuracy of decision-making, and to use Dezert-Smarandache Theory (DSmT) theory for uncertainty reasoning so as to increase the discrimination degree of decision support probability.

To sum up, the main contributions of this paper are as follows.

1) According to the analysis of the loom mechanical equipment and weaving principle, the dynamic model of the main shaft of the rapier loom is established, and the monitoring data collection position and type of the loom state monitoring are clarified through the model. In addition, this paper proposes that the loom state analysis can be based on the warp tension of the loom and the commonly used vibration data.
2) Aiming at the problem of many reduction results when the rough set method is directly applied to loom attribute data processing, this paper proposes a genetic multi-objective optimization method fused with the genetic algorithm. The method uses the genetic algorithm to improve the reduction step in the rough set method to optimize the reduction result and improve the classification accuracy of the system decision.
3) Aiming at the problem of matching multiple rules for new objects in the rough set method, this paper proposes to use DSmT theory combined with rough set theory to carry out uncertainty reasoning and increase the distinguishability of decision support probability.

In order to verify the feasibility and effect of the method proposed in this paper, a step-by-step comparison experiment and a system experiment on an actual rapier loom are carried out in this paper. The loom condition monitoring mapping network can obtain a better identification effect and improve the performance of the loom condition monitoring system.

II. DYNAMIC MODEL OF LOOM SPINDLE

In this section, the structure and weaving process of the loom are analyzed, the dynamic model of the loom is constructed, and the monitoring data source of the condition monitoring system is determined accordingly.

A. WEAVING PRINCIPLE OF LOOM

A rapier loom can be divided into five significant mechanisms: opening, weft insertion, beating-up, let-off and coiling. The mechanical structure of the rapier loom is shown in Fig. 1. Different angles of the weaving machine spindle correspond to different weaving process processes, which is the core of the weaving machine operation. Fig. 2 shows a table of the spindle position angles of the weaving machine when performing different processes.

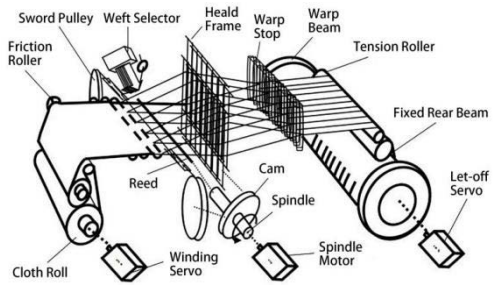

FIGURE 1. Mechanical structure diagram of rapier loom.

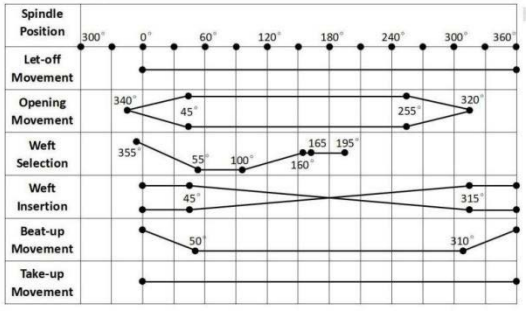

FIGURE 2. Position angle table of loom moving spindle.

The mechanical transmission relationship of the rapier loom spindle is shown in Fig. 3. The primary motor

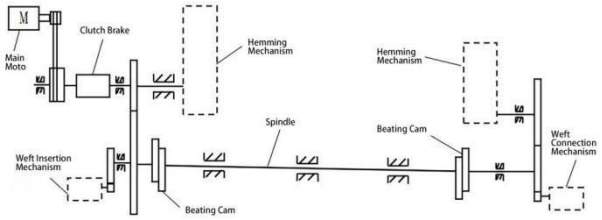

FIGURE 3. Transmission system diagram of rapier loom.

transmits the power to the weaving machine spindle through the belt pulley, brake clutch system, and reduction gear to drive the weaving machine spindle movement. The primary shaft drives the wefting cam to complete the wefting process.

B. SPINDLE DYNAMICS MODEL

The main shaft of the loom is formed by a series of mass elements, beam elements, and support elements connected one after another in the form of a chain-like structure. It is convenient and practical to use the transfer matrix method to analyze and calculate the vibration system of this form [32]. The dynamic model diagram of the spindle of the rapier loom is shown in Fig. 4.

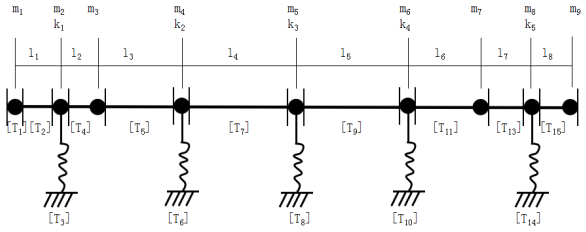

FIGURE 4. Dynamic model diagram of rapier loom spindle.

As shown in Fig. 4, the loom spindle system is decomposed into several relatively simple subsystems with a single degree of freedom. The state vectors represent the generalized forces and generalized displacements on the connected end faces of each subsystem, and the transfer matrix is used to represent the relationship from the input end of the system to the output end. The primary shaft system of the loom is calculated according to the concentrated mass point, beam and support point separately.

When the system performs simple harmonic motion since m_i is a rigid body, its left and right lateral displacements y are equal, which can be expressed as:

$$y_i^R = y_i^L \tag{1}$$

The rotation angle θ on the left and right sides of m_i is equal, which is expressed as:

$$\theta_i^R = \theta_i^L \tag{2}$$

m_i is a large volume part whose rotational inertia cannot be neglected. Thus, the bending moment of the subsystem can be expressed as:

$$M_i^R = M_i^L - J_i\omega^2\theta_i^L \tag{3}$$

The sheer force transfer relationship between the left and right sides of the subsystem can be expressed as:

$$Q_i^R = Q_i^L + m_i\omega^2 y_i^L \tag{4}$$

In these equations, the R and L superscripts indicate the location of the parameters (i.e., the right or left side of the subsystem), M is the bending moment received by the subsystem, J is its moment of inertia, ω is the angular frequency of system motion, and Q is the shear force experienced by the subsystem. Therefore, the state transfer relationship between the left and right sides of m_i can be expressed as:

$$\begin{bmatrix} y \\ \theta \\ M \\ Q \end{bmatrix}_i^R = \begin{bmatrix} 1 & 0 & 0 & 0 \\ 0 & 1 & 0 & 0 \\ 0 & -J\omega^2 & 1 & 0 \\ m_i\omega^2 & 0 & 0 & 1 \end{bmatrix}_i \begin{bmatrix} y \\ \theta \\ M \\ Q \end{bmatrix}_i^L \tag{5}$$

which can be abbreviated as:

$$[z]_i^R = [P]_i[z]_i^L \tag{6}$$

where $[P]_i$ is called the point transfer matrix of the concentrated mass point m_i.

Denote beams with l_i. Separating l_i from the system and ignoring the mass of the beam itself, the transfer relationship of the bending moment on the beam is as follows based on a balance of forces:

$$M_i^L = M_{i-1}^R + Q_{i-1}^R l_i \tag{7}$$

The shear force transfer relationship of the beam is:

$$Q_i^L = Q_{i-1}^R \tag{8}$$

The force analysis of beam l_i uses the left end point of the beam as the coordinate origin, the radial direction of the beam is the x direction, and the tangential direction is the y direction. According to the mechanics of materials, we know:

$$M = EI\frac{d\theta}{dx} \tag{9}$$

where E is the elastic modulus of the beam, and I is the moment of inertia of the beam. From the set relation, we know:

$$y = \int \theta dx \tag{10}$$

Therefore, the angle transfer relationship between the left and right ends of the beam is:

$$\theta_i^L = \theta_{i-1}^R + \frac{1}{(EI)_i}\int_0^{l_i} M_i^L dx \tag{11}$$

The lateral displacement transfer relationship between the left and right ends of the beam is:

$$y_i^L = y_i^R + \int_0^{l_i} \theta_i^L dx \tag{12}$$

The left end rotation angle of the middle beam on the right side of (12) is represented by the rotation angle of the right endpoint of its adjacent subsystem, and it is substituted into (11) to obtain:

$$\theta_i^L = \theta_{i-1}^R + \frac{M_{i-1}^R l_i}{(EI)_i} + \frac{Q_{i-1}^R l_i^2}{2(EI)_i} \tag{13}$$

The rotation angle of the left end of the beam is expressed by the lateral displacement of the right end point of its adjacent subsystem and is substituted into (12) to obtain:

$$y_i^R = y_{i-1}^R + \theta_{i-1}^R l_i + \frac{l_i^2}{2(EI)_i} M_{i-1}^R + \frac{l_i^3}{6(EI)_i} Q_{i-1}^R \tag{14}$$

Equations (7), (8), (13), and (14) can be represented in matrix form as:

$$\begin{bmatrix} y \\ \theta \\ M \\ Q \end{bmatrix}_i^L = \begin{bmatrix} 1 & l & \frac{l^2}{2EI} & \frac{l^3}{6EI} \\ 0 & 1 & \frac{l}{EI} & \frac{l^2}{2EI} \\ 0 & 0 & 1 & l \\ 0 & 0 & 0 & 1 \end{bmatrix}_i \begin{bmatrix} y \\ \theta \\ M \\ Q \end{bmatrix}_{i-1}^R \tag{15}$$

which can be abbreviated as:

$$[z]_i^L = [F]_i [z]_{i-1}^R \tag{16}$$

where $[F]_i$ is the field transfer matrix of massless beam segment l_i. Using (5) for ideal rigid points and (15) for ideal massless beams, the state vector relationship model of each point from the left end to the right end of the system can be established.

Assuming that the equivalent stiffness of the support point m_i is k, the equivalent viscous damping coefficient is ζ, and the concentrated mass of the support is m_i, the displacement relationship between the left and right sides of the support point is:

$$y_i^R = y_i^L \tag{17}$$

Therefore, the transfer relationship of the state vectors on the left and right sides of the support point of m_i is:

$$\theta_i^R = \theta_i^L \tag{18}$$

The bending moment relationship is expressed as:

$$M_i^R = M_i^L \tag{19}$$

The shear force relationship is expressed as:

$$Q_i^R = Q_i^L + (m_i\omega^2 - i\xi\omega - k) y_i^L \tag{20}$$

Therefore, the transfer relationship of the state vectors on the left and right sides of the support point is:

$$\begin{bmatrix} y \\ \theta \\ M \\ Q \end{bmatrix}_i^R = \begin{bmatrix} 1 & 0 & 0 & 0 \\ 0 & 1 & 0 & 0 \\ 0 & 0 & 1 & 0 \\ m_i\omega^2 - i\xi\omega - k & 0 & 0 & 1 \end{bmatrix}_i \begin{bmatrix} y \\ \theta \\ M \\ Q \end{bmatrix}_i^L \tag{21}$$

TABLE 1. Mechanical parameters of loom spindleits for magnetic properties.

parameter	value	unit
l1	64	mm
l2	134	mm
l3	173	mm
l4	850	mm
l5	906	mm
l6	115	mm
l7	108	mm
l8	64	mm
m1	6.64	kg
m2	1.86	kg
m3	9.94	kg
m4	5.89	kg
m5	9.58	kg
m6	6.24	kg
m7	10.24	kg
m8	1.86	kg
m9	5.48	kg
k1	2.431	105N/mm
k2	3.564	105N/mm
k3	2.433	104N/mm
k4	3.059	104N/mm
k5	2.437	105N/mm
E	2.06	105N/mm2
ω	340	rad/s
J1	3.839	105 kg·mm2
PI	3.14	--
d	54	mm

which can be abbreviated as:

$$[z]_i^R = [T]_i [z]_i^L \tag{22}$$

where $[T]_i$ is the transfer matrix of the state vectors on both sides of the support point.

According to the structure of the main shaft of the rapier loom and the working principle of the loom, using the parameters listed in Table 1, the dynamic model of the main shaft of the rapier loom is established.

Thus, the input from one end of the primary shaft can be transmitted to any position of the primary shaft, and the

natural frequency and primary vibration shape of the primary shaft of the loom can be calculated.

III. DATA PROCESSING AND FUSION OF THE STATE DETECTION SYSTEM

Because many of the data collected on the loom are incomplete and uncertain, these data cannot be directly used for decision-making on the loom status [33], [34]. The collected data must be preprocessed before the data are fused to construct a rough set decision table.

A. LOOM STATE FEATURE DESCRIPTION AND DATA PREPROCESSING

The fluctuation characteristics of the warp tension of the loom can describe the working state of the opening mechanism, the beating-up mechanism, and the roll feeding system. The primary vibration of the loom mechanical equipment can systematically reflect the overall operation state of the equipment. Therefore, this system focuses on the fluctuation of the warp tension. Data and body vibration data are processed as source data, and a decision table is constructed.

1) CHARACTERISTIC DESCRIPTION OF THE WARP TENSION FLUCTUATION OF LOOMS

The warp yarn tension data of the loom sampled by the sensor is represented only by the function $y_i = f(t_i)$ $(i = 0, 1, \ldots, n)$ of a series of points t_i in the corresponding time interval. In order to evaluate the fluctuation characteristics of warp tension, it is necessary to estimate the function value corresponding to any time node. This system selects the cubic spline interpolation method to solve the approximation function of the warp tension fluctuation curve of the loom. Because all the weaving actions of the loom are performed based on the spindle position angle, the spindle position angle is selected as the independent variable of the warp tension fluctuation function of the loom, and the definition domain is [0, 360).

The interpolation curve of the warp tension fluctuation composed of the warp tension of the loom in one cycle is shown in Fig. 5, which indicates that the interpolation effect of 49 interpolation nodes is better than that of 24 interpolation nodes. Also, the cubic spline interpolation curve using 49 interpolation nodes can more accurately describe the measured fluctuation of warp tension on the loom and the nature of the curve. Therefore, in the onboard condition monitoring system of the loom, six attributes of the three extreme point positions of the 49-point interpolation curve, the relative stability interval of the tension, and the mean value of the tension sampling points are selected to describe the warp tension fluctuation of the loom.

2) CHARACTERISTIC DESCRIPTION OF THE VIBRATION SIGNAL OF THE LOOM SPINDLE

From the analysis of the weaving principle of the loom above, we can see that the main shaft of the loom is the power source of the weaving mechanism, and its vibration can reflect the condition of the entire loom. The vibration of the main shaft

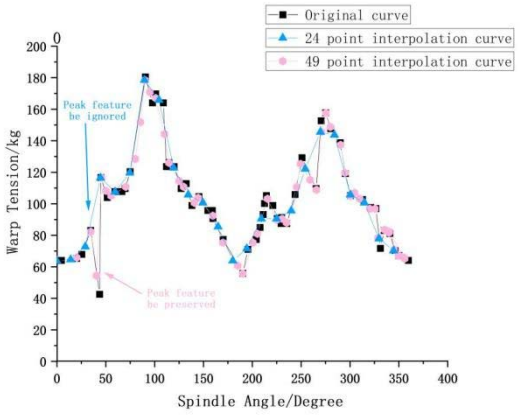

FIGURE 5. Loom warp tension collection circuit.

of the loom can be obtained by measuring the vibration of the journals at both ends of the main shaft. The sensor used in this paper is an IEPE acceleration sensor. The physical diagram of the journals and the sensor at both ends is shown in Fig. 6.

FIGURE 6. The journals and sensors at both ends of the loom spindle.

In engineering practice, spectrum analysis is often used to analyze vibration signals. The time-domain diagram of the main shaft vibration signal and the corresponding spectrum analysis diagram of the loom in the normal weaving state are shown in Fig. 7.

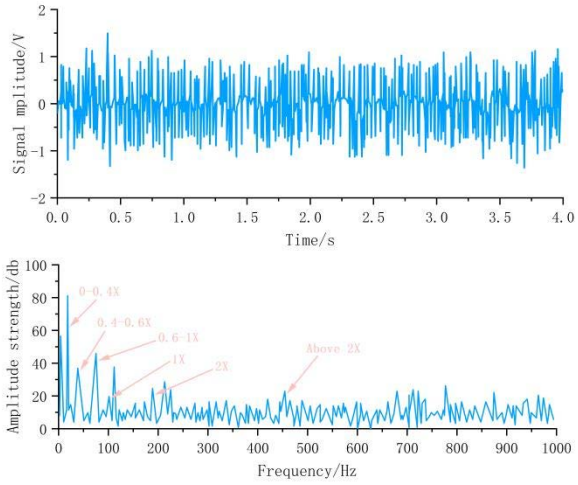

FIGURE 7. Time-domain and frequency-domain diagrams of spindle vibration signals.

The operating speed of the main shaft is generally below 10 r/s, that is, below 10 Hz. Therefore, the fundamental

frequency of vibration of the main shaft of the loom is below 10 Hz. The operating speed of the spindle is called the fundamental frequency of the spindle, denoted as X. Taking the spindle fundamental frequency X as the unit, the vibration generated by the spindle has multiple harmonics in addition to 1 times the spindle fundamental frequency 1X. The failure of the loom is often reflected in the multiple harmonics. Below 1X is the sub-low-frequency area, 1X to 10X is the low-frequency area, and above 10X is the high-frequency area. If the amplitude in the sub-low-frequency region is high, the fault types include oil swirl and so on. If the amplitude in the low-frequency region is high, the fault types are unbalance, misalignment, looseness, etc. If the amplitude in the high-frequency region is high, the gear bearing is often faulty, such as wear, cracks, etc. In this paper, the vibration signal of the main shaft is divided into six attributes according to the amplitude: 0∼0.4X, 0.4∼0.6X, 0.6∼1X, 1X, 2X and greater than 2X. Since there are two measurement points of the spindle vibration, the left journal and the right journal, there are 12 attributes to describe the spindle vibration signal. The vibration attribute table of the main shaft of the loom is shown in Table 2.

TABLE 2. Loom spindle vibration description attribute table.

Measuring point	Attributes	attribute value	Measuring point	Attributes	attribute value
Left	0~0.4X	{High, Medium, Low}	Right	0~0.4X	{High, Medium, Low}
Left	0.4~0.6X	{High, Medium, Low}	Right	0.4~0.6X	{High, Medium, Low}
Left	0.6~1X	{High, Medium, Low}	Right	0.6~1X	{High, Medium, Low}
Left	1X	{High, Medium, Low}	Right	1X	{High, Medium, Low}
Left	2X	{High, Medium, Low}	Right	2X	{High, Medium, Low}
Left	Above 2X	{High, Medium, Low}	Right	Above 2X	{High, Medium, Low}

B. CONSTRUCTION AND REDUCTION OF THE ROUGH SET DECISION TABLE

After data collection, key feature extraction, data preprocessing, etc., a rough set decision table can be constructed, and the decision table can be reduced.

1) CONSTRUCTION OF THE ROUGH SET DECISION TABLE

Assuming that the loom state feature monitoring system contains five first-generation attribute items, denoted as $A = \{a_1, a_2, a_3, a_4, a_5\}$, the definition set can be denoted $V = \{V_1, V_2, V_3, V_4, V_5\}$, where V_i is the attribute A set of values for a_i, $i = 1, 2, \ldots, 5$. The function $f : ai \text{ —> } Vi$ represents the relationship between the attribute a_i and its value. The existing state instance set U is collected according to the first-generation attribute items. According to rough set theory, the loom state monitoring information system can be expressed as $IS = \langle U, A, V, f \rangle$.

Considering the identification of the spindle wear degree as an example, we let the attribute a_1 represent the wear degree of the loom spindle, where $V_1 = \{\text{severe, slight, normal}\}$; the attribute a_2 represents the measured value of the weft yarn tension in a certain weaving cycle, which is divided into five levels as $V_2 = \{2, 1, 0, -1, -2\}$; attribute a_3 represents the weaving performance of the loom at a certain stage, and the weaving performance of the loom is divided into four types, where $V_3 = \{\text{excellent, good, medium, poor}\}$; and attributes a_4 and a_5 are other parameter attributes of the loom. The resulting decision table is shown in Table 3.

TABLE 3. Example of decision representation in spindle wear identification.

state instance (U)	Condition property (C)				decision attributes (D)
	a2	a3	a4	a5	a1
x1	1	0 (Excellent)	2	2	1 (severe)
x2	2	1 (Good)	2	1	2 (marginal)
x3	-2	0 (Excellent)	0	2	2 (marginal)
x4	1	3 (Difference)	1	1	1 (severe)
x5	-1	2 (middle)	0	0	3 (normal)
x6	0	0 (Excellent)	2	1	3 (normal)
x7	1	0 (Excellent)	3	1	2 (marginal)
x8	1	3 (Difference)	1	1	2 (marginal)

For the loom parameter monitoring problem, the loom weft tension monitoring decision table is constructed as shown in Table 4.

TABLE 4. Example of decision-making in weft tension parameter monitoring.

state instance (U)	Condition property (C)				decision attributes (D)
	a1	a3	a4	a5	a2
x1	1 (severe)	0 (Excellent)	2	2	1
x2	2 (marginal)	1 (Good)	2	1	2
x3	2 (marginal)	0 (Excellent)	0	2	-2
x4	1 (severe)	3 (Difference)	1	1	1
x5	3 (normal)	2 (middle)	0	0	-1
x6	3 (normal)	0 (Excellent)	2	1	0
x7	2 (marginal)	0 (Excellent)	3	1	1
x8	2 (marginal)	3 (Difference)	1	1	1

2) REDUCTION OF ROUGH SET DECISION TABLES

After the rough set decision table is constructed, the attribute reduction of the information system can be carried out. The core idea of attribute reduction is to reduce redundant attributes and obtain attribute reduction subsets according to the size of attribute dependence or importance without affecting the classification and decision-making ability of the decision information table. Attribute reduction of

information systems can maintain the classification ability of the information system and simplify the system's expression and optimize the system's operational performance. This paper adopts a heuristic attribute reduction algorithm based on attribute importance. The algorithm first finds the kernel of the decision-making system, then calculates the importance of each conditional attribute and adds it to the attribute set according to specific requirements until the set is a reduction.

In the information system IS $= \langle U, A, V, f\rangle$, if the indistinguishable relation induced by attribute set A is equal to the indistinguishable relation induced by its subset, then IND(A) = IND(A − {a}). Then, attribute a is a redundant attribute of attribute set A, and the process of eliminating redundant attributes in the attribute set is called knowledge reduction. An information system can have multiple attribute reductions, and the intersection of all reductions is called the core of the information system. Attribute reduction of information systems can maintain the classification ability of the information system and simplify the system's expression and optimize the system's operational performance.

In the onboard condition monitoring system of the loom, some attributes make only small contributions to the loom state decision and can even lead to the wrong state decision; thus, these irrelevant and misleading attributes must be eliminated. In the information system IS $= \langle U, C, D, V, f\rangle$, the importance of attribute a relative to decision attribute D based on attribute set B can be determined by the following equation:

$$\mathrm{SIG}_{\gamma}(a, B, D) = \gamma_{B\cup\{a\}}(D) - \gamma_{B}(D) \tag{23}$$

where SIGr(a, B, D) describes the contribution of attribute a to decision attribute set D based on conditional attribute set B: the larger the value is, the more important attribute a is to decision-making. The heuristic attribute reduction algorithm flow based on attribute importance is shown in Fig. 8.

The reduction algorithm based on attribute importance is applied to decision table 3, and the reduction result is:

1) Attribute set $C_{a11} = \{a_3, a_4, a_5\}$;
2) Attribute set $C_{a12} = \{a_2, a_4\}$;
3) Attribute set $C_{a13} = \{a_2, a_3, a_5\}$;

Similarly, the reduction result of decision Table 4 is:

1) Attribute set $C_{a21} = \{a_1, a_3, a_5\}$;
2) Attribute set $C_{a22} = \{a_1, a_4\}$;
3) Attribute set $C_{a23} = \{a_3, a_4, a_5\}$;

C. MACHINE LEARNING GENERALIZATION PERFORMANCE CONTROL

Because an industrial site where data are collected is typically noisy, this decision-making algorithm may lead to overfitting. In order to ensure more reliable state monitoring results, the reduction results of rough set methods need to be improved. According to the structural risk minimization (SRM) principle, to reduce the structural risk of the rough set method, both empirical risk and confidence range must be minimized concurrently. However, empirical risk minimization and confidence range minimization are often contradictory. Therefore, the structural risk control of the rough set method is a typical multiobjective optimization problem, and there are multiple relative optimal solutions. Under the premise of not deteriorating other goals, these solutions can only ensure that one or a few core goals that are most concerned are optimal.

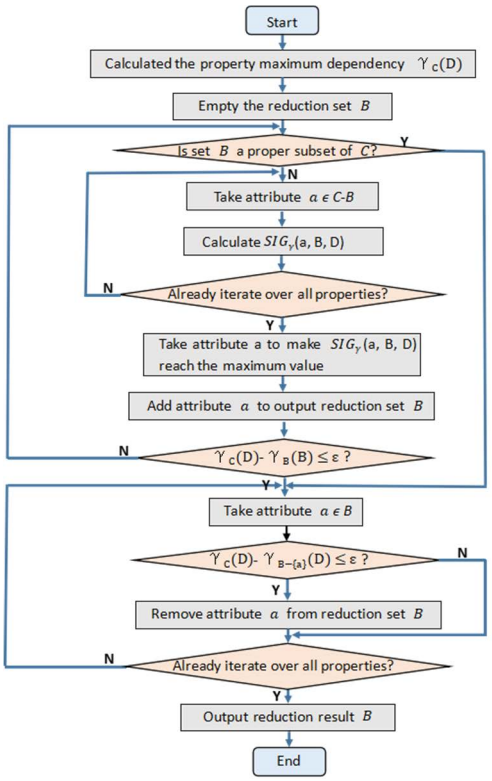

FIGURE 8. Flow chart of the rough set attribute reduction algorithm.

1) EMPIRICAL RISK CONTROL ALGORITHM BASED ON GENETIC MULTIOBJECTIVE OPTIMIZATION

A genetic algorithm is a computational model of an optimization problem that simulates Darwin's natural evolution process. It has been widely used in machine learning, neural network, optimal control and other fields. It has the characteristics of a flexible search process, wide application range, global optimization ability and high optimization process efficiency. In this paper, the genetic multi-objective optimization method is used to optimize the reduction steps of the rough set method.

The application steps of the genetic algorithm can be summarized as follows:

1) Determination of the initial population: we encode the candidate solutions in the feasible domain, randomly select a part as the first generation encoding group, and then calculate the fitness of each encoding concurrently;
2) Selection operation: Similar to natural evolution, the selection mechanism of the genetic algorithm should ensure that individuals with high fitness are more easily selected. Usually, the probability of an individual being

selected can be described as:

$$P_i = \frac{h_i}{\sum_{i=1}^{n} h_i} \tag{24}$$

3) Crossover and mutation operation: The crossover operator selects some bits of the two individual samples of the population to generate the next generation of individuals by random exchange, and the mutation operator randomly reverses a specific bit in the individual samples. Typically, crossover and mutation should be applied concurrently to avoid prematurely trapping the algorithm into a local optimum.
4) Optimal population output: We repeat this process of selection, mutation, and crossover until the end condition is met, and the new generation of the population obtained is the optimal solution set found by the algorithm.

When applying the genetic algorithm, selection, inheritance, and mutation operations are standard processes, but the coding process and fitness evaluation must be designed according to different applications. When using the genetic algorithm to evaluate the structural risk of the attribute subset of the decision table, each condition attribute subset is regarded as a candidate solution and coded. The coding rule is as follows: when the ith condition attribute in the decision table is included in the subset condition attribute subset, the ith bit of the code is 1; otherwise, it is 0.

Fitness describes the individual's contribution to the optimization goal, and a suitable fitness evaluation mechanism is the key to the success of the genetic algorithm. When using the genetic algorithm to control the structural risk of the rough set method, the empirical risk corresponding to the conditional attribute subset is defined as:

$$f_B = 1 - \gamma_B(D) \tag{25}$$

The algorithm flow for obtaining the fitness of the candidate solution is shown in Fig. 9.

2) PERFORMANCE TEST OF THE GENETIC OPTIMIZATION ROUGH SET METHOD

In order to verify the effectiveness of the empirical risk control algorithm based on multiobjective genetic optimization, 10 UCI datasets were used for testing. Table 5 shows the classification accuracy of the conventional rough set method for each UCI dataset when the threshold is 0.95, the attribute importance index parameter is 0.5, as well as the classification accuracy of the algorithm using the multiobjective genetic optimization empirical control method.

The experimental results show that the rough set method optimized by the genetic algorithm more easily obtains high classification accuracy with different datasets.

3) EXAMPLE OF ATTRIBUTE REDUCTION BASED ON GENETIC MULTIOBJECTIVE OPTIMIZATION

The reduction with the smallest number of attributes is typically considered the best reduction. However, not all the reductions of decision tables have only a unique reduction result with the smallest number of attributes. In order to choose the best reduction result of the decision table, the empirical risk control algorithm based on multiobjective genetic optimization is used to evaluate the fitness of Tables 3 and 4, and the results are shown in the following table.

1) The selection basis of the attribute reduction results of decision Table 3 is shown in Table 6.
2) The selection basis of the attribute reduction results of decision Table 4 is shown in Table 7.

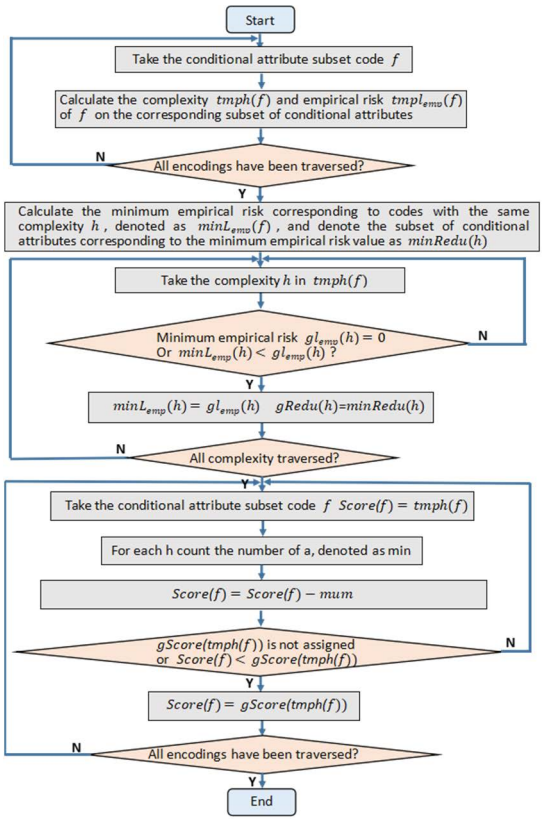

FIGURE 9. Flow chart of the attribute subset empirical risk assessment algorithm of the rough set method.

TABLE 5. Classification accuracy obtained by the rough set method.

Dataset	Conventional Rough Set Method	Optimized Rough Set Method
Hepatitis	0.8775	0.9163
Ionosphere	0.9201	0.9429
Soybean	0.9253	0.9282
Image Segmentation	0.8714	0.8714
Credit Approval	0.8246	0.8341
Cloud	0.8041	0.8252
Wine	0.9549	0.9386
Flags	0.6389	0.6555
Automobile	0.7917	0.7645
Zoo	0.9418	0.9518
Average value	0.8550	0.8629

TABLE 6. Selection basis of reduced attributes for spindle wear identification.

Attribute subset (B)	encoded value	Complexity	empirical risk	Domination sort value
{a2, a3, a4, a5}	1111	137.4109	0	5
{a2, a3, a4}	1110	45.8036	0	4
{a2, a3, a5}	1101	34.3527	0	3
{a2, a4, a5}	1011	34.3527	0	3
{a3, a4, a5}	0111	22.9018	0	2
{a2, a3}	1100	11.4509	0.2857	9
{a2, a4}	1010	11.4509	0	1
{a2, a5}	1001	8.5882	0.2857	8
{a3, a4}	0110	7.6339	0.2857	7
{a3, a5}	0101	5.7255	0.5714	12
{a4, a5}	0011	5.7255	0.2857	6
{a2}	1000	2.8627	0.4286	10
{a3}	0100	1.9085	0.5714	11
{a4}	0010	1.9085	0.7143	13
{a5}	0001	1.4314	0.8571	14

TABLE 7. Selection basis of reduced attributes for weft tension parameter monitoring.

Attribute subset (B)	encoded value	Complexity	empirical risk	Domination sort value
{a1, a3, a4, a5}	1111	112.0538	0	4
{a1, a3, a4}	1110	37.3513	0	3
{a1, a3, a5}	1101	28.0134	0	2
{a1, a4, a5}	1011	28.0134	0	2
{a3, a4, a5}	0111	37.3513	0	3
{a1, a3}	1100	9.3378	0.2857	6
{a1, a4}	1010	9.3378	0	1
{a1, a5}	1001	7.0034	0.2857	5
{a3, a4}	0110	12.4504	0.2857	7
{a3, a5}	0101	9.3378	0.5714	9
{a4, a5}	0011	9.3378	0.2857	6
{a1}	1000	2.3345	0.8571	11
{a3}	0100	3.1126	0.5714	8
{a4}	0010	3.1126	0.7143	10
{a5}	0001	2.3345	0.8571	11

After evaluation, the best-reduced attribute set of decision Table 3 is $C_{a12} = \{a_2, a_4\}$, and the best-reduced attribute set of decision Table 4 is $C_{a22} = \{a_1, a_4\}$. In addition, if the risk of taking an attribute value is relatively high, the order of the decision attribute rule set can be appropriately adjusted according to the dominant order value.

IV. JUDGMENT AND DECISION-MAKING METHOD OF MONITORING SYSTEM STATUS

A. EXTRACTION METHOD OF DECISION RULES BASED ON ROUGH SET THEORY

After attribute reduction is completed, decision rules can be constructed by reducing attribute sets and attribute values. After processing by the rough set rule extraction algorithm, the corresponding relationship between the condition attribute and the decision attribute of the information system is shown in Fig. 10.

For information system IS $= \langle U, C, D, V, f\rangle$, we let its attribute reduction result B be the proper subset of attribute set C, U/B means classify U according to B set, U/D means

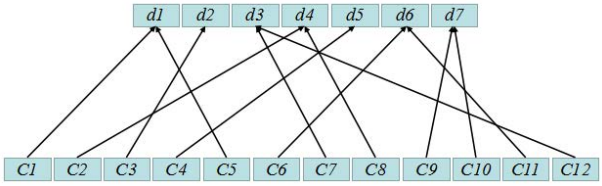

FIGURE 10. Schematic diagram of the relationship between the pre rule and post rule of the rough set decision rule.

that U is classified according to D set, X belongs to U/B, and Y belongs to U/D. Thus, the decision rule of the information system can be expressed as:

$$DES(X, B) \Longrightarrow DES(Y, D) \tag{26}$$

where DES(X, B) is called the rule antecedents, which is the condition part of the rule; DES(Y, D) is called the rule consequences, which is the decision part of the rule; and DES(X, B) is defined as:

$$DES(X, B) = \wedge(a = f(x, a)), \quad x \in X,\ a \in B \tag{27}$$

where a = f(x, a) represents the essential elements of the class description.

Due to data inconsistency and uncertainty, there may be a deterministic or possible relationship between rule antecedents and rule posteriors. According to generalization decision theory, the objects with the same generalization decision value in the universe are divided into the same set K. If the generalization decision of an object subset K is $|\delta B(x)| = 1$, then all objects in K can be accurately classified under the knowledge level given by B. If the generalization decision of the object subset K is $|\delta B(x)| > 1$, then all objects in K cannot be accurately classified under the knowledge level given by B. The generalization decision of object x in U concerning attribute set B is defined as:

$$\delta_B(x) = \{v_i | f(y, x) = v_i, y \in [x]_B\} \tag{28}$$

where v_i is the decision attribute. Therefore, the rough set method's minimum rule set extraction algorithm flow is shown in Fig. 11.

In order to obtain the best classification accuracy, it should be ensured that a smaller set of rules is obtained when the decision rules are extracted. The following takes the spindle wear identification and weft tension parameter monitoring as examples to extract the minimum ruleset.

1) The rule set extracted from decision Table 3 is shown in Table 8.
2) The rule set extracted from decision Table 4 is shown in Table 9.

B. UNCERTAINTY REASONING

When there is a new object for rule matching, three situations may occur:

(1) The new object matches only one rule.
(2) The new object matches multiple rules.
(3) The new object does not match any rules.

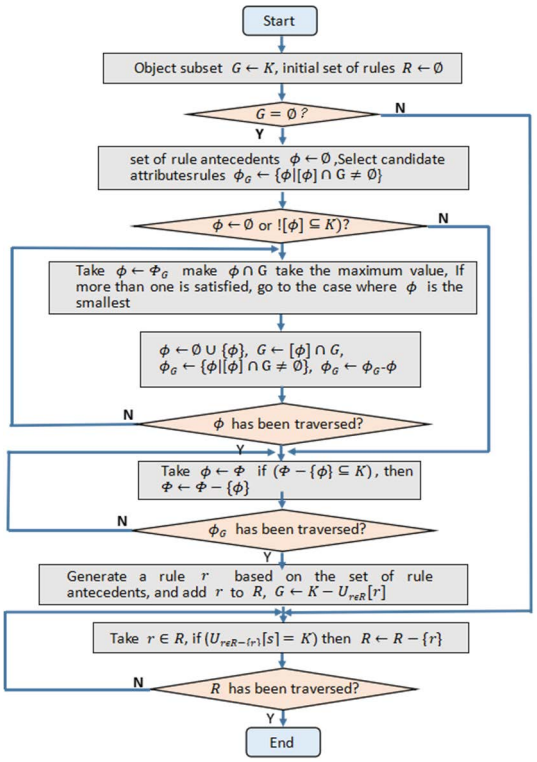

FIGURE 11. Rough set rule extraction process based on attribute importance evaluation.

TABLE 8. Minimum rule set extraction in spindle wear identification.

Number	Rules (reduced to a_2, a_4)	Support	Credibility
1	a2(-2) ∧ a4(0) => d(2)	0.125	1
2	a2(-1) ∧ a4(0) => d(3)	0.125	1
3	a2(0) ∧ a4(2) => d(3)	0.125	1
4	a2(1) ∧ a4(2) => d(1)	0.125	1
5	a2(2) ∧ a4(2) => d(2)	0.125	1
6	a2(1) ∧ a4(1) => d(1)	0.125	0.5
7	a2(1) ∧ a4(3) => d(2)	0.125	1
8	a2(1) ∧ a4(1) => d(2)	0.125	0.5

TABLE 9. Minimum rule set extraction in weft tension parameter monitoring.

Number	Rules (reduced to a_1, a_4)	Support	Credibility
1	a1(1) => d(1)	0.25	1
2	a1(2) ∧ a4(2) => d(2)	0.125	1
3	a1(2) ∧ a4(0) => d(-2)	0.125	1
4	a1(3) ∧ a4(0) => d(-1)	0.125	1
5	a1(3) ∧ a4(2) => d(0)	0.125	1
6	a1(2) => d(1)	0.25	1

Case (1) can directly determine decision-making attributes, and case (3) can typically be converted into the case (1) or (2) using the partial rule matching method. In case (2), the most common method is to score the support of each matching rule for the new object and then select the rule with the most considerable support for the decision of the new object.

1) UNCERTAINTY REASONING METHOD BASED ON DSmT THEORY

The new object can infer the decision attribute value by matching the rules in the rule base. However, when the new instance matches a nondeterministic rule with credibility lower than 1, the unique decision attribute value cannot be obtained. In order to deal with the uncertainty of system rule matching, this paper incorporates the DSmT uncertainty inference method. In this application, the recognition framework of DSmT is a collection of new object matching rules, defined as:

$$U = \{\theta_1, \theta_2, \ldots, \theta_n, \} \tag{29}$$

The superpower set DU generated by the union and intersection of elements in the identification frame satisfies the following conditions:

1) $\phi, \theta_1, \theta_2, \ldots, \theta_n \in D^U$.
2) If sets A and B belong to the superpower set DU, then the intersection and union of A and B also belong to DU;
3) Only if the elements satisfy conditions (1) and (2) do they belong to DU;

For the recognition frame U, define a function m(A) ——> [0, 1], where A is a subset of U, if the function m satisfies:

$$\begin{cases} m(\phi) = 0 \\ \sum_{A \subset U} m(A) = 1 \end{cases} \tag{30}$$

Then, m(A) is called the basic probability assignment of A, which represents the exact degree of confidence in proposition A. The trust function on U is defined as:

$$BEL(A) = \sum_{B \subset A} m(B) \quad (\forall A \subset B) \tag{31}$$

The function BEL(A) represents the total trust of A. The likelihood function that defines the recognition frame U is:

$$PL(A) = 1 - BEL(\bar{A}) \tag{32}$$

where PL(A) represents the degree of trust of A. When three rules are initially matched, the description of the implementation process of the DSmT-based rule uncertainty inference method is shown in Fig. 12.

2) EXAMPLE OF UNCERTAINTY REASONING FOR LOOM CONDITION MONITORING

Taking the uncertainty rules 6 and 8 in Table 8 as examples, the decision rule matching reasoning is carried out.

1) We let the new instance be as shown in Table 10.
2) According to the rule matching method, instance x_k matches rules 6 and 8 in table 8, and its corresponding decision attributes may be $d_1 = 1$ and $d_2 = 2$; thus, the identification framework for determining the target is $U = \{d_1, d_2\}$. Then, the superpower set is:

$$D^U = \{\phi, d_1, d_2, d_1 \cap d_2, d_1 \cup d_2, \} \tag{33}$$

In the information table, the proportion of support of the rule, the prior probability of the value of the decision attribute, and the proportion of the value of attributes a_3

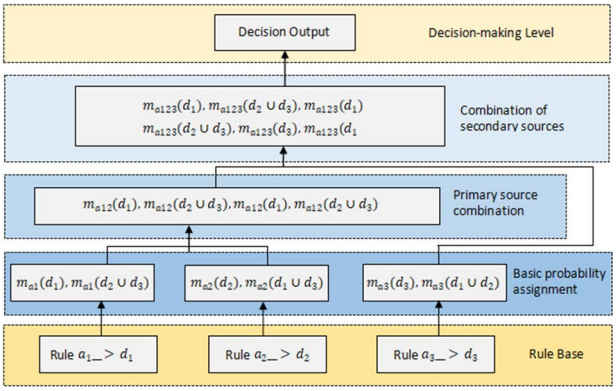

FIGURE 12. Rule uncertainty reasoning method based on DSmT.

TABLE 10. New examples of spindle wear identification.

state instance (U)	Condition property (C)			
	a2	a3	a4	a5
xk	1	0 (Excellent)	1	1

and a_5 are taken as the fundamental probability value of target recognition: $m_1(d_1) = 0.5$, $m_1(d_2) = 0.5$, $m_2(d_1) = 0.19$, $m_2(d_2) = 0.8$, $m_2(d_1 \cap d_2) = 0.01$, $m_3(d_1) = 0.33$, $m_3(d_2) = 0.67$, $m_4(d_1) = 0.25$, and $m_4(d_2) = 0.75$. Combining these rules scoring methods yields $m_a = m_1 \oplus m_2$, and thus, $m_a(d_1) = 0.1980$ and $m_a(d_2) = 0.8020$; $m_b = m_3 \oplus m_4$, and then, $m_b(d_1) = 0.1410$ and $m_b(d_2) = 0.8590$, which leads to $m_c = m_a \oplus m_b$. Thus, $m_c(d_1) = 0.0389$ and $m_c(d_2) = 0.9611$.

3) Therefore, the trust function is $Bel(d_1) = 0.0389$, $Bel(d_2) = 0.9611$. These calculations indicate that various rule evaluation methods can be integrated through fusion, which can markedly increase the discrimination of decision support probability. If a threshold is introduced, the decision value of the newly added objects listed above can be determined to be d_2.

V. TEST OF THE ON-BOARD CONDITION MONITORING SYSTEM OF LOOMS

A. LOOM STATE DATA COLLECTION TEST

The onboard condition monitoring platform of the loom collects data according to the characteristics of the first generation and simultaneously displays data of different sampling frequencies. After analyzing the data collected by the loom's analog quantity, the loom's average spindle speed is 330.01 RPM, which is near the actual system setting. Also, the maximum deviation is 1.01 RPM, and the relative error is less than 0.31%, which meets the measurement requirements of the spindle speed of the loom. Similarly, the relative errors of other analog acquisition parameters of the system are calculated, and the relative errors can be lower than 0.35%. The set values of the loom parameters and the calculation results of the relative error are shown in Table 11.

TABLE 11. Effectiveness analysis of loom condition monitoring data acquisition.

Attributes	set value	sample average	maximum value	minimum	maximum deviation	Relative error
Rotating speed	330.00	330.01	330.75	328.99	1.01	0.31
humidity	--	26.73	26.79	26.64	0.14	0.34
temperature	--	31.58	31.65	31.48	0.10	0.32
warp tension	110.00	110.00	110.25	109.66	0.34	0.31
oil temperature	--	32.11	32.18	32.01	0.10	0.31
effectiveness	--	87.00	87.20	86.73	0.27	0.31
Cutter current	--	4.23	4.24	4.22	0.02	0.28
Braking distance	--	474.99	476.08	473.54	2.54	0.30

TABLE 12. Comparison of spindle wear recognition rates of on-board condition monitoring methods for looms.

Number	Recognition rate of traditional rough set method	Improve the recognition rate of rough set method
1	99.5	100
2	100	100
3	99	99.5
4	98.5	100
5	98	99
6	100	100
7	98.5	100
8	99.5	99.5
9	100	100
10	100	100
Average recognition rate	99.955	99.998

According to the index of the attribute data in the table, it can be known that the data sampling results of each attribute item of the monitoring system can genuinely reflect the actual situation of the loom parameters. The system can also realize real-time synchronization of loom state characteristic data, providing data support for state reasoning.

B. RECOGNITION RATE TEST OF THE ONBOARD CONDITION MONITORING SYSTEM OF LOOMS

In order to test the effect of the proposed loom on-board condition monitoring method, taking the identification of main shaft system wear as an example, the system was installed on two looms of the same model with different degrees of wear. The loom state data were collected for 1000 seconds, respectively. The 2000 data instances are randomly divided into ten groups, each containing 200 data instances. Table 12 compares recognition rates between the decision network constructed by the traditional rough set method and the decision network constructed by the improved rough set method.

The above test experiments on the recognition rate of spindle wear show that the average recognition rate of the loom state mapping network constructed by the traditional rough set method for spindle wear is 99.955%; after improvement, the average recognition rate can reach 99.998%. Compared with the traditional rough set method, the genetic multi-objective optimization and DSmT improved rough set method have a better recognition effect on the loom state decision.

VI. CONCLUSION

This paper presents a decision method for condition monitoring of high-speed rapier loom systems, mainly improving the attribute reduction step and the decision matching step of the traditional rough set method. A spindle dynamics model is developed for the spindle, the core of the weaving process, and a table of weaving machine spindle parameters are summarised to identify the sources of weaving machine monitoring data. The addition of warp vibration monitoring is proposed to improve the monitoring system's decision accuracy and compensate for the lack of data sources for conventional weaving machine monitoring. The data is analyzed using the rough set method. For discontinuous data types in the time domain, the data are first pre-processed using interpolation methods, which give a complete picture of warp tension fluctuations. For the problem of complex loom attribute data and the unclear association between data content and decision making, the rough set method is used for processing. Experiments show that the loom attribute data can be effectively extracted using the rough set method from the loom state decision rules. However, the pure rough set method suffers from weak machine generalization and uncertain rules for matching new objects. In order to improve the generalization performance of machine learning, this paper proposes a genetic multi-objective optimization method incorporating the rough set method with a genetic algorithm, in which each conditional attribute subset of the decision table is treated as a candidate solution encoded. The genetic algorithm is applied to evaluate the structural risk of the attribute subset of the decision table to construct a weaving machine state decision rule base with a good recognition effect and high decision accuracy. In order to reduce the uncertainty of matching rules for new objects, this paper proposes a rough set method incorporating the uncertainty derivation method of DSmT to assign basic probabilities and two-level source combinations to the rules that may match so as to derive the decision with the highest accuracy, and experiments show that this method increases the discrimination of decision support probabilities. Finally, the condition monitoring system is tested on a actual loom. The experimental test shows that the average recognition rate of the spindle wear problem is 99.955% with the loom state mapping network constructed by the traditional rough set method. After the rough set method is improved by genetic algorithm and DSmT theory, the average recognition rate of spindle wear identification is 99.998%. Compared with the traditional rough set method, the improved rough set method can achieve better recognition results for the weaving machine monitoring mapping network. Overall, this paper proposes a series of improvements and implementations for condition monitoring of high-speed rapier weaving machines, hopefully providing some reference for researchers in this field.

REFERENCES

[1] L. Ma and X. Wang, "Technical progress of weaving equipment from ITMA 2019," *Textile Herald*, vol. 12, pp. 18–29, 2019.

[2] G. Vladimir, B. Dmitriy, T. N. Win, and I. Evgen, "The vision system in the weaving loom industry," in *Proc. IEEE Conf. Russian Young Researchers Elect. Electron. Eng. (EIConRus)*, Feb. 2017, pp. 669–671.

[3] P. J. Priya, "PIC based power loom automation for weaving in textile industries," in *Proc. IEEE Int. Conf. Electron., Comput. Commun. Technol. (CONECCT)*, Bangalore, India, Jul. 2020, pp. 1–6, doi: 10.1109/CONECCT50063.2020.9198451.

[4] D. Dong and Z. Shi, "The loom monitoring system design with high reliability and easy maintainability," in *Proc. Int. Conf. Control, Automat. Syst. Eng. (CASE)*, Jul. 2011, pp. 1–5.

[5] K. Sun and Y. Yao, "Development of real-time monitoring software system for warp knitting machine production process," *Prog. Textile Sci. Technol.*, vol. 7, pp. 32–34, 2018.

[6] Y. Jiang, X. Han, and M. Wang, "Application of active real-time database technology in power grid condition monitoring," *Microcomput. Appl.*, vol. 37, no. 8, pp. 127–129 and 139, 2021.

[7] H. Li, Y. Xiao, and F. Peng, "Application of online condition monitoring system based on stress wave technology in ladle turntable," *Metall. Automat.*, vol. 45, no. 5, pp. 79–85, 2021.

[8] Y. Zhang, "A brief discussion on the application of stress wave detection technology in fault diagnosis of polyolefin granulation unit," *China Equip. Eng.*, vol. 13, pp. 169–170, 2021.

[9] Z. Han *et al.*, "Research on the monitoring sensing system of military cross-river bridge equipment," *Equip. Manuf. Technol.*, vol. 7, pp. 66–71, 2021.

[10] F. Shen, Q. Huang, and S. Wang, "Research on equipment condition monitoring and fault diagnosis based on laser interferometry," *Automat. Instrum.*, vol. 6, pp. 123–127, 2021.

[11] M. Caporuscio, F. Flammini, N. Khakpour, P. Singh, and J. Thornadtsson, "Smart-troubleshooting connected devices: Concept, challenges and opportunities," *Future Gener. Comput. Syst.*, vol. 111, pp. 681–697, Oct. 2020.

[12] L. Zhang *et al.*, "Condition monitoring and fault diagnosis system of high-power hydromechanical transmission," *Comput. Meas. Control*, vol. 30, no. 1, pp. 15–19 and 25, 2022.

[13] K. Ding *et al.*, "Application research of online condition monitoring in power system," *Times Agricult. Machinery*, vol. 46, no. 7, pp. 38–39 and 44, 2019.

[14] X. Gao *et al.*, "Research on online status monitoring technology of virtual circuit in smart substation based on comprehensive evaluation and identification method," *Power Syst. Protection Control*, vol. 47, no. 3, pp. 182–187, 2019.

[15] J. Cong, "Online monitoring and condition maintenance technology of electrical equipment," *Electron. Technol. Softw. Eng.*, vol. 22, pp. 229–230, 2019.

[16] Y. Wang *et al.*, "Intelligent monitoring technology of ship shafting based on edge computing," *Chin. J. Weaponry Equip. Eng.*, vol. 42, no. 8, pp. 287–291, 2021.

[17] B. Ding *et al.*, "Research on security condition monitoring technology of power information system based on big data analysis," *Elect. Meas. Instrum.*, vol. 58, no. 11, pp. 59–66, 2021.

[18] Y. Ren and K. Zhang, "Comprehensive condition monitoring and fault diagnosis technology of wind turbine drive chain," *Chin. J. Drainage Irrigation Mech. Eng.*, vol. 36, no. 7, pp. 613–616 and 631, 2018.

[19] D. Li *et al.*, "Research on condition monitoring technology of wind turbine gearbox based on likelihood learning machine," *Chin. J. Sol. Energy*, vol. 42, no. 4, pp. 374–379, 2021.

[20] S. Chen, "Research on fault diagnosis of rapier loom bearings with wavelet neural network," Tech. Rep., 2022, vol. 8.

[21] Q. Zhang, J. Huang, and Y.-T. Gao, "Fault diagnosis method and application of power converter based on variational mode decomposition combined with kernel density," in *Proc. Chin. Automat. Congr. (CAC)*, Nov. 2019, pp. 2059–2063.

[22] S. Zhang, Z. Liu, S. He, J. Wang, and L. Chen, "Improved double TQWT sparse representation using the MQGA algorithm and new norm for aviation bearing compound fault detection," *Eng. Appl. Artif. Intell.*, vol. 110, Apr. 2022, Art. no. 104741.
[23] D. Zhang, Z. Ning, B. Yang, T. Wang, and Y. Ma, "Fault diagnosis of permanent magnet motor based on DCGAN-RCCNN," *Energy Rep.*, vol. 8, pp. 616–626, 2022.
[24] P. Zhang, T. Li, G. Wang, C. Luo, H. Chen, J. Zhang, D. Wang, and Z. Yu, "Multi-source information fusion based on rough set theory: A review," *Inf. Fusion*, vol. 68, pp. 85–117, Apr. 2021.
[25] Q. Zhang, Q. Xie, and G. Wang, "A survey on rough set theory and its applications," *CAAI Trans. Intell. Technol.*, vol. 1, no. 4, pp. 323–333, 2016.
[26] V. Muralidharan and V. Sugumaran, "Rough set based rule learning and fuzzy classification of wavelet features for fault diagnosis of monoblock centrifugal pump," *Measurement*, vol. 46, no. 9, pp. 3057–3063, 2013.
[27] W. H. Wang, K. D. Liu, D. H. Zhou, and C. H. Wang, "A fuzzy and rough sets integrated approach to fault diagnosis," *IFAC Proc. Volumes*, vol. 35, no. 1, pp. 245–250, 2002.
[28] M. Suo, L. Tao, B. Zhu, Y. Chen, C. Lu, and Y. Ding, "Soft decision-making based on decision-theoretic rough set and Takagi–Sugeno fuzzy model with application to the autonomous fault diagnosis of satellite power system," *Aerosp. Sci. Technol.*, vol. 106, Nov. 2020, Art. no. 106108.
[29] C. Rajeswari, B. Sathiyabhama, S. Devendiran, and K. Manivannan, "A gear fault identification using wavelet transform, rough set based GA, ANN and C4.5 algorithm," *Proc. Eng.*, vol. 97, pp. 1831–1841, Jan. 2014.
[30] M. Hu, E. C. C. Tsang, Y. Guo, D. Chen, and W. Xu, "A novel approach to attribute reduction based on weighted neighborhood rough sets," *Knowl.-Based Syst.*, vol. 220, May 2021, Art. no. 106908.
[31] J. Xie, B. Q. Hu, and H. Jiang, "A novel method to attribute reduction based on weighted neighborhood probabilistic rough sets," *Int. J. Approx. Reasoning*, vol. 144, pp. 1–17, May 2022.
[32] J. C. Junhong, "Optimal design of the main shaft of a rapier loom considering dynamics," M.S. thesis, Hefei Univ. Technol., Hefei, China, 2002.
[33] W. Liu *et al.*, "Big data tagging system and key technologies of power equipment operating status," *China Electr. Power*, vol. 55, no. 1, pp. 126–132, 2022.
[34] Y. Li, "Research on data preprocessing based on rough set theory," M.S. thesis, Harbin Univ. Sci. Technol., Harbin, China, 2008.

WEILING LIU received the bachelor's and master's degrees in mechanical engineering from the Hebei University of Technology, in 1995 and 1998, respectively, and the Ph.D. degree from Tianjin University, in 2006.

From 2009 to 2011, she conducted postdoctoral research with Bao Jingling at the Tianjin Academy of Environmental Sciences. She is currently an Associate Professor with the Hebei University of Technology. Her main research interests include artificial intelligence and automation control.

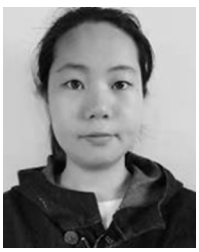

PING LIU received the graduate degree from the Hebei University of Technology, in 2020, where she is currently pursuing the master's degree. Her research interests include intelligent control and health management.

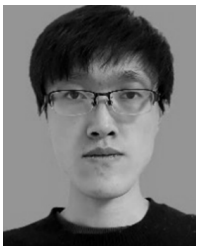

XIAOLIANG WANG is currently pursuing the master's degree in electronic information with the Hebei University of Technology. His research interests include embedded technology and intelligent control.

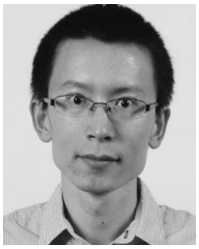

ZHAOZONG MENG (Member, IEEE) received the B.S. degree in measurement and control technology and instrument from Sichuan University, Chengdu, China, in 2006, the M.S. degree from Beihang University, Beijing, China, in 2009, and the Ph.D. degree in computer science from the University of Huddersfield, West Yorkshire, U.K., in 2014.

From 2014 to 2016, he was a Research Associate with The University of Manchester, and from 2016 to 2018, he was a Research Fellow with the University of Southampton. Since 2018, he has been a Lecturer with the School of Mechanical Engineering, Hebei University of Technology, Tianjin, China. Since 2020, he has been promoted an Associate Professor. His research interests include advanced sensor techniques, wearable devices and body area networks, manufacturing intelligence, the Industrial IoT, and cyber-physical systems.

YUNFENG JIANG is currently pursuing the Ph.D. degree. He is also an Associate Researcher. His research interests include new perception and intelligent control.

YANJUN XIAO received the bachelor's degree in industrial automation and the master's degree in mechanical design and manufacturing and automation from the Hebei University of Technology, in 2000 and 2009, respectively. From 2001 to 2007, he worked with the Central Laboratory, School of Mechanical Engineering, Hebei University of Technology, where he has been a Professor with the School of Mechanical Engineering, since 2017. He is currently teaching with the School of Mechanical Engineering, Hebei University of Technology, where he is also working with the Tianjin Key Laboratory of Power Transmission and Safety Technology for New Energy Vehicles. He is a professional with Jiangsu Career Leader Company Ltd. His main research interests include waste heat recovery and industrial control. His awards and honors include the title of "Three Three Three" Three-Level Talent in Jiangsu Province, in 2018, the 2017 and 2019 Hebei Science and Technology Invention Award, and the honorary title of the "Hebei Science and Technology Talent," in 2017.